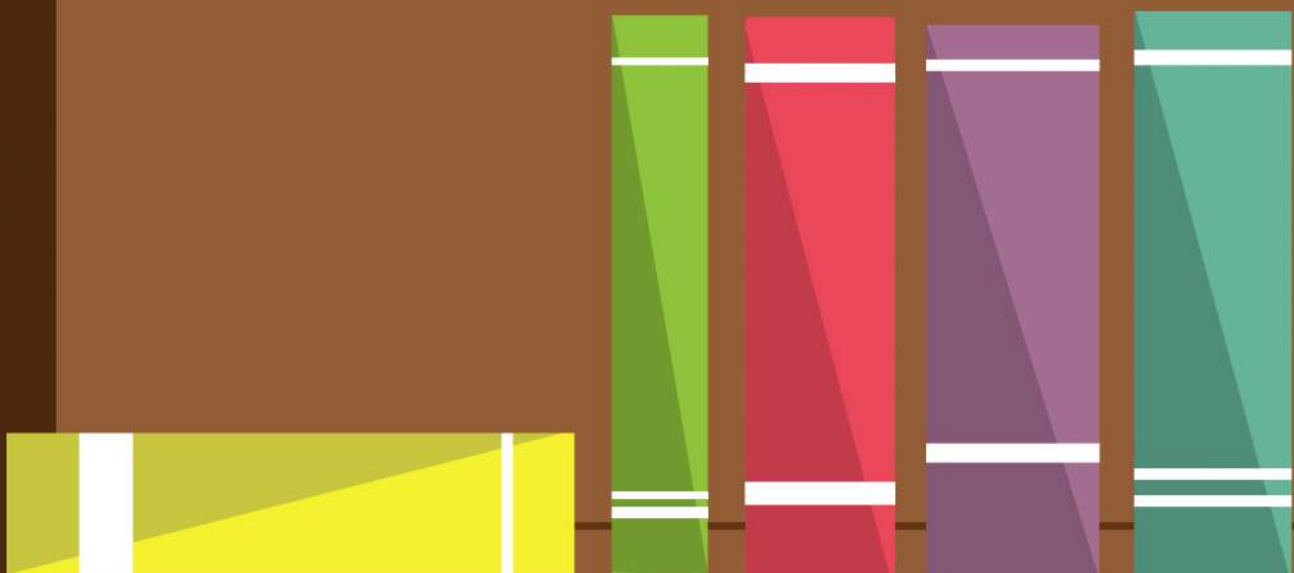
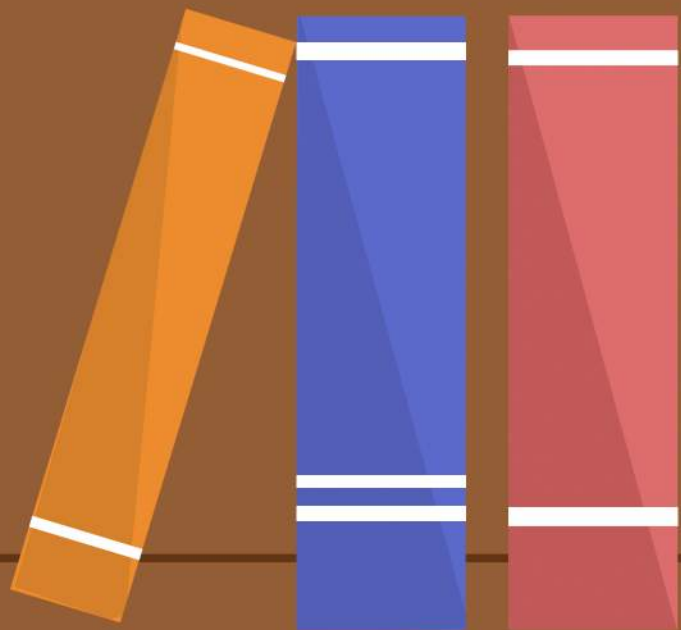




บทความย่อผลงานวิจัยที่ได้รับการตีพิมพ์
ในวารสารและการประชุมระดับชาติและนานาชาติ
คณะวิทยาศาสตร์ มหาวิทยาลัยศรีนครินทรวิโรฒ
ประจำปี 2556



ภาควิชาฟิสิกส์

NO₂-sensing properties of WO₃ nanorods prepared by glancing angle DC magnetron sputtering

M. Horprathum, K. Limwichean, A. Wisitsoraat, P. Eiamchai, K. Aiempnanakit, P. Limnonthakul,
N. Nuntawong, V. Pattantsetakul, A. Tuantranont, and P. Chindaudom

ที่มา: Sensors and Actuators B Chemical. 2013. 176 : 685–691

In this work, the NO₂-sensing properties of the tungsten trioxide (WO₃) nanorods prepared by dc magnetron sputtering with glancing-angle deposition (GLAD) technique are comparatively studied with that of WO₃ thin film deposited by normal sputtering process. The crystal structure and morphologies were characterized by grazing-incidence X-ray diffraction and field emission scanning electron microscopy, respectively. As-deposited WO₃ structure deposited at glancing angle of 85° exhibited amorphous crystal structure with uniform isolated columnar nanorod morphology with average length, diameter and spacing between nanorods of around 400 nm, 50 nm and 10 nm, respectively. Annealing at 400 and 500 °C resulted in polycrystalline phase and more porous nanorod network with very large effective surface area. The NO₂ sensing response of WO₃ nanorods was found to be higher than that of WO₃ thin film by a factor of 2-5 depending on operating temperature and gas concentration. In addition, WO₃ nanorod annealed at 500 °C exhibited an optimum response of ~27-2.0 ppm of NO₂ at 250 °C. Therefore, GLAD using reactive dc magnetron sputtering has been demonstrated as a practical method for fabrication of well-aligned metal oxide nanostructures and is potential for gas-sensing applications.

Effects of Precursor Concentration on Hexagonal Structures of ZnO Nanorods Grown by Aqueous Solution Method

P. Limnonthakul, C. Chananonwathorn, K. Aiempakit, J. Kaewkhao,
P. Eiamchai, M. Horprathum

ที่มา: Advanced Materials Research. 2013. 770: 120-123

The ZnO nanorods were fabricated on top of the seeded gold layer by the aqueous solution method with the solution of zinc nitrate and hexamethylenetetramine (HTMA) at 90°C for 24 hours. The variety of the ZnO nanorods were prepared and investigated based on the precursor concentrations, in a range of 1 to 40 mM. The physical morphologies and crystal structures were characterized by field-emission scanning electron microscopy (FE-SEM) and X-ray diffractometry (XRD), respectively. The results showed that, with the small precursor concentrations, the lateral growth of the nanorods was highly significant when compared to their axial growth. The precursor concentration of 20 mM was best optimized for the preparation of the ZnO nanorod arrays with the hexagonal structures at the highest rod diameter and length. At the higher concentrations, although the nanorod size remained nearly constant, the length was however rapidly decreased. Further analyses also proved that, with the increased precursor concentrations, the number density of the ZnO nanorods was progressively increased along with the more complete hexagonal wurtzite structures.

Description of low temperature bandtail states in two-dimensional semiconductors using path integral approach

Udomsilp Pinsook, Anusit Thongnum and Virulh Sa-yakanit

ที่มา: Appl. Phys. Lett. 2013. 102: 162101

We used the solutions from the variational path integral to suggest a function form of the bandtail states of a two-dimensional system. The analytic solutions provide two regimes, i.e., the ground state (low temperature) and the semiclassical (high temperature) limits. We used the theoretical results to describe the results of the bandtail states in Si/SiO₂ heterostructure reported recently (Jock *et al.*, Appl. Phys. Lett. **100**, 023503 (2012)). The low-temperature bandtail provided good agreement to the experimental results (sample B) with the parameters of $\Delta = 0.225$ nm, $L = 3.55$ nm, and $a = 5$ nm.

Phase Transition and Dielectric Properties of PNNZT-BNLT Ceramics

Pichitchai Butnoi, Nuttapon Pisitpipathsin, Puripat Kantha,
Patamas Bintachitt, and Kamonpan Pengpat

ที่มา: *Ferroelectrics*. 2013. 452 (1): 1-6

The $(1-x)\text{Pb}(\text{Ni}_{0.33}\text{Nb}_{0.67})_{0.5}\text{Ti}_{0.35}\text{Zr}_{0.15}\text{O}_3$ [PNNZT] - $x\text{Bi}_{0.4871}\text{Na}_{0.4871}\text{La}_{0.0172}\text{TiO}_3$ [BNLT] ceramics ($x = 0, 0.03, 0.06, 0.09, 0.12$ and 0.15) were prepared by a two steps mixed-oxide method. XRD patterns of all ceramic samples exhibited a complete perovskite phase without pyrochlore and no second phase. The BNLT addition has a significant effect on the grain growth inhibition of PNNZT-BNLT ceramics. The dielectric studies indicated that the phase transition behavior of the ceramic compositions becomes more diffuse with increasing BNLT content. The addition of BNLT content caused the increase in T_m , for example: about 16% for the 0.03 mol% BNLT sample while $\tan\delta$ was reduced to about 60% compared with that of pure PNNZT sample.

NO₂-sensing properties of WO₃ nanorods prepared by glancing angle DC magnetron sputtering

M. Horprathum, K. Limwichean, A. Wisitsoraat, P. Eiamchai, K. Aiempnanakit, P. Limnonthakul, N. Nuntawong, V. Pattantsetakul, A. Tuantranont, and P. Chindaudom

ที่มา: Sensors and Actuators B Chemical. 2013. 176 : 685–691

In this work, the NO₂-sensing properties of the tungsten trioxide (WO₃) nanorods prepared by dc magnetron sputtering with glancing-angle deposition (GLAD) technique are comparatively studied with that of WO₃ thin film deposited by normal sputtering process. The crystal structure and morphologies were characterized by grazing-incidence X-ray diffraction and field emission scanning electron microscopy, respectively. As-deposited WO₃ structure deposited at glancing angle of 85° exhibited amorphous crystal structure with uniform isolated columnar nanorod morphology with average length, diameter and spacing between nanorods of around 400 nm, 50 nm and 10 nm, respectively. Annealing at 400 and 500 °C resulted in polycrystalline phase and more porous nanorod network with very large effective surface area. The NO₂ sensing response of WO₃ nanorods was found to be higher than that of WO₃ thin film by a factor of 2-5 depending on operating temperature and gas concentration. In addition, WO₃ nanorod annealed at 500 °C exhibited an optimum response of ~27-2.0 ppm of NO₂ at 250 °C. Therefore, GLAD using reactive dc magnetron sputtering has been demonstrated as a practical method for fabrication of well-aligned metal oxide nanostructures and is potential for gas-sensing applications.

Effects of Precursor Concentration on Hexagonal Structures of ZnO Nanorods Grown by Aqueous Solution Method

P. Limnonthakul, C. Chananonwathorn, K. Aiempakit, J. Kaewkhao,
P. Eiamchai, M. Horprathum

ที่มา: Advanced Materials Research. 2013. 770: 120-123

The ZnO nanorods were fabricated on top of the seeded gold layer by the aqueous solution method with the solution of zinc nitrate and hexamethylenetetramine (HTMA) at 90°C for 24 hours. The variety of the ZnO nanorods were prepared and investigated based on the precursor concentrations, in a range of 1 to 40 mM. The physical morphologies and crystal structures were characterized by field-emission scanning electron microscopy (FE-SEM) and X-ray diffractometry (XRD), respectively. The results showed that, with the small precursor concentrations, the lateral growth of the nanorods was highly significant when compared to their axial growth. The precursor concentration of 20 mM was best optimized for the preparation of the ZnO nanorod arrays with the hexagonal structures at the highest rod diameter and length. At the higher concentrations, although the nanorod size remained nearly constant, the length was however rapidly decreased. Further analyses also proved that, with the increased precursor concentrations, the number density of the ZnO nanorods was progressively increased along with the more complete hexagonal wurtzite structures.

Description of low temperature bandtail states in two-dimensional semiconductors using path integral approach

Udomsilp Pinsook, Anusit Thongnum and Virulh Sa-yakanit

ที่มา: Appl. Phys. Lett. 2013. 102 :162101(1-4)

We used the solutions from the variational path integral to suggest a function form of the bandtail states of a two-dimensional system. The analytic solutions provide two regimes, i.e., the ground state (low temperature) and the semiclassical (high temperature) limits. We used the theoretical results to describe the results of the bandtail states in Si/SiO₂ heterostructure reported recently (Jock *et al.*, Appl. Phys. Lett. **100**, 023503 (2012)). The low-temperature bandtail provided good agreement to the experimental results (sample B) with the parameters of $\Delta = 0.225$ nm, $L = 3.55$ nm, and $a = 5$ nm.

Phase Transition and Dielectric Properties of PNNZT-BNLT Ceramics

Pichitchai Butnoi, Nuttapon Pisitpipathsin, Puripat Kantha,
Patamas Bintachitt, and Kamonpan Pengpat

ที่มา: *Ferroelectrics*. 2013. 452 (1): 1-6

The $(1-x)\text{Pb}(\text{Ni}_{0.33}\text{Nb}_{0.67})_{0.5}\text{Ti}_{0.35}\text{Zr}_{0.15}\text{O}_3[\text{PNNZT}] - x\text{Bi}_{0.4871}\text{Na}_{0.4871}\text{La}_{0.0172}\text{TiO}_3[\text{BNLT}]$ ceramics ($x = 0, 0.03, 0.06, 0.09, 0.12$ and 0.15) were prepared by a two steps mixed-oxide method. XRD patterns of all ceramic samples exhibited a complete perovskite phase without pyrochlore and no second phase. The BNLT addition has a significant effect on the grain growth inhibition of PNNZT-BNLT ceramics. The dielectric studies indicated that the phase transition behavior of the ceramic compositions becomes more diffuse with increasing BNLT content. The addition of BNLT content caused the increase in T_m , for example: about 16% for the 0.03 mol% BNLT sample while $\tan\delta$ was reduced to about 60% compared with that of pure PNNZT sample.

Upper Bound for the Ground State Energy of Fermionic Matter in 2D
ขอบเขตบนของพลังงานที่สถานะพื้นของสสารประเภทเฟอร์มิออนในสองมิติ

Supanya Boonprasit, Pisuttawan Sripirom Sirininlakul and Siri Sirininlakul
สุปัญญา บุญประสิทธิ์ พิศุทธรวรรณ ศรีภิรมย์ สิรินิลกุล และ สิริ สิรินิลกุล

ที่มา: วารสารวิทยาศาสตร์ มศว. 2556. 29(2) : 121-129

We derive the upper bound for the exact ground-state energy involving a single power of the number of electrons in matter, N . The bound is based on the following construction. We consider the N electrons localized in k non-overlapping ordered squares size $2L \times 2L$, with the k nuclei placed at the centers of each square area with appropriate choices of trial wavefunction for the N electrons.

Quasinormal Modes of the Reissner-Nordstrom Black Holes with the
Sectional Curvature, $k = -1, 0$, และ 1 , in the 5-Dimensional Anti de Sitter
Spacetime

ควอซีนอร์มอลโหมดของหลุมดำไรส์เนอร์-นอร์ดสเตริมที่มีค่าความโค้ง
ส่วนย่อย $k = -1, 0$, และ 1 ในปริภูมิเวลาแอนไทเดอซีเตอร์ 5 มิติ

Jaroonsak Jarassriwilai and Suphot Musiri.

จรูญศักดิ์ จรัสศรีวิลไล และ สุพจน์ มุสิริ

ที่มา: วารสารวิทยาศาสตร์ มศว. 2556. 29(2) : 159-173

Quasinormal modes of the Reissner-Nordstrom black hole in 5-dimensional AdS spacetimes are analytically calculated. The black holes are perturbed by a charged and massive scalar field. The scalar field charge is coupled to the Maxwell field from the black holes. We vary the sectional curvature as $k = -1, 0$ and 1 . The results are similar to those in [5, 6], for 4-dimensional cases. We also approximate some small-value terms at the infinity to check the error from the analytical approximation. The higher value number n of quasinormal modes and their frequencies, the lesser error-value numbers are found.

The Synthesis of Bissulfonamide Derivation for Fluoride Sensor

การสังเคราะห์อนุพันธ์บิสซัลโฟนาไมด์สำหรับตรวจจับฟลูออไรด์

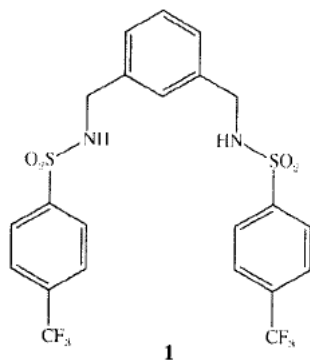
Phitchaya Muensri, Pan Tongraung, Ratchanok Pingaew, Kem Pumsa-ard and Piyada

Jittangprasert

พิชญ่า หมั่นศรี, แพน ทองเรือง, รัชนก ปิ่นแก้ว, เข้ม พุ่มสะอาด และ ปิยะดา จิตรตั้งประเสริฐ

ที่มา: วารสารวิทยาศาสตร์ มศว. 2556. 29(1) : 83-94

A new anion sensor, 1,3-bis[(*p*-trifluoromethylphenylsulfonamido)methyl]benzene (**1**), bearing sulfonamide group as binding unit and *p*-trifluoromethylbenzene group as signaling unit was readily synthesized in high percentage yield. The structure of the ligand **1** was characterized by IR, ¹H NMR, ¹³C NMR and Mass spectrometry. The complexation with various anions including F⁻, Cl⁻, I⁻, H₂PO₄⁻ and CH₃COO⁻ was studied by UV-visible spectrophotometry in dimethyl sulfoxide solution. The results indicated that the ligand **1** has high selectivity for fluoride over other anions (F⁻ >> CH₃COO⁻, H₂PO₄⁻, Cl⁻ and I⁻). Moreover, the absorption spectrum obviously changed with appearance of a new band at 295.5 nm. The stoichiometry of complex between the ligand **1** and fluoride was 1:2. The binding constant of the complex by fitting the UV-visible titration data was (1.10 ± 0.07) × 10⁷ M⁻². The interaction of the ligand **1** with F⁻ was also studied by ¹H NMR titration experiments. The results showed the deprotonation of sulfonamide protons which induced upfield shifts of aromatic protons.



The Preparation and Characterization of Superconductor Y358

การเตรียมและการวัดสมบัติของตัวนำยวดยิ่ง Y358

**Praweena Artsamai, Suppunyou Meakniti, Sarunya Aromsawang, Tunyanop Nilkamjon,
Suppadate Sujinapram, Sermsuk Ratreng, Thitipong Kruaehong and Pongkaew
Udomsamuthirun**

**ประวีณา อากสมัย, สัพพัญญู เมฆนिति, ศรัณญา อารมย์สว่าง, ชัญชนพ นิลกำจร, ศุภเดช สุจินพรัหม, เสริมสุข
รัตเรง, ฐิติพงษ์ เครือหงส์, ปิยะมาศ ไชยนอก, และ พงษ์แก้ว อุดมสมุทรหิรัญ**

ที่มา : วารสารวิทยาศาสตร์ มศว. 2556. 29(1) : 111-120

In this research, we synthesized and characterize the physical properties of Y358 superconductor by solid state reaction. The raw materials Y_2O_3 (99.99%) $BaCO_3$ (99.9%) and CuO (99+%) were mixed, ground and react in air at $950^\circ C$ and annealing $500^\circ C$ were done. The sample obtained had the density of 4.97 g/cm^3 . In this research, we made the resistivity measurement set that was characterized for suitable condition for critical temperature measure. We found that the critical temperature was 93 K, with grain size about $20 \mu\text{m}$. The crystal structure was orthorhombic with $a = 3.83839 \text{ \AA}$, $b = 3.88058 \text{ \AA}$ and $c = 31.12290 \text{ \AA}$.

The technique of Viscosity Measurement by Falling Sphere:
Role of Wall Effect
เทคนิคการวัดความหนืดโดยอาศัยการตกของวัตถุทรงกลม: บทบาทของ
อิทธิพลของผนังหลอด

Hataichanok Phetmatsri, Tunyanop Nilkamjon and Supitch Khemmani

หทัยชนก เพ็ชรมาตศรี ชัยนพ นิลกำจร และ สุพิชญ์ แคมมณี

ที่มา : วารสารวิทยาศาสตร์ มศว. 2556. 29(2) : 131-148

In this thesis, the principle of uncertainty in measurement is used rigorously to investigate the experiment of falling sphere in Newtonian fluids containing in cylindrical tubes. The experiment is done by using various sizes of sphere and cylindrical tube so that the wall effect factor can be determined. In this experiment, our invented fluid with appropriate viscosity is used so that any space variation of falling sphere is easily captured by human eyes. As a result, a stop clock controlled by a human can be used to detect any time duration of the sphere moving within an interval by acceptable uncertainty in measurement. Moreover, the rotational viscometer (Brookfield) is used here to measure the viscosity of the fluid up to 20 rpm of the rotational frequency. The experimental result of the wall effect factors are in good agreement with theory proposed by Haberman and Sayre, where the factor is the function of the ratio of sphere diameter to cylindrical tube diameter, except some of our ratio settings.

One of advantages of the wall effect is that it allows us to measure the viscosity of glycerin by this simple falling sphere experiment. Without the wall effect, the sphere falls too fast so that human eyes capture leads to a huge uncertainty in measurement. By choosing the sphere diameter of about 4 mm and the (inner) cylindrical tube diameter of about 4.48 mm, the know wall effect factor from our experiment can then be used to calculate the viscosity of glycerin which is 782 ± 49 cps at 24 °C. This result does not differ significantly from the one obtained by Brookfield viscometer, i.e. 722.3 ± 6.0 cps at the same temperature. However, it is clear in this case that the uncertainty associated with falling sphere technique is about 8 times of the one associated with Brookfield viscometer.